Finite element simulations of the bending of the IPMC sheet

D. Pugal[a,b], H. Kasemägi[a], K. J. Kim[b], M. Kruusmaa[a], A. Aabloo[a]

[a]Institute of Technology, Tartu University, Estonia
[b]Active Materials and Processing Laboratory, Mechanical Engineering Department, University of Nevada, Reno, NV, U.S.A

ABSTRACT

This paper presents a electro-mechanical model of an IPMC sheet. The model is developed using Finite Element method. The physical bending of an IPMC sheet due to the drift of counter-ions (e.g Na+) and water in applied electric field are simulated. Our model establishes a cause-effect relationship between the charge imbalance of the counter-ions and the mechanical bending of the IPMC sheet. The model takes into account the mechanical properties of the Nafion polymer as well as the platinum coating. As the simulations are time dependent, a transient model is used and some additional parameters, such as damping coefficients, are included. In addition to electro-mechanical model, electrochemical reactions are introduced. Equations describing periodic adsorption and desorption of CO and OH on a platinum electrode of an IPMC muscle immersed into formaldehyde solution are coupled to mechanical properties of the proposed model. This permits us to simulate self-oscillatory behavious of an IPMC sheet. The simulation results are compared to experimental data.

Keywords: Electroactive polymers, EAP, IPMC, Finite Element method, Electrochemical-mechanical analysis, Actuator, Coupled problem, Self-oscillating systems

1. INTRODUCTION

EAP-based electromechanical actuators are valuable for use in a number of applications from micro robotics to military and space applications. These actuators are light weight, noiseless, mechanically simple; have large displacement and good damage tolerance which makes it possible to use them as artificial muscles. In this paper we consider simulations of ionic polymer-metal composite[1] (IPMC) materials with the Finite Element method (FEM).

IPMC materials are highly porous polymer materials such as Nafion^{TM}, Teflon, filled with some kind of ionic conductive liquid. There are water based IPMCs which operate in aquatic environment and current is caused by ions such as Na+, K+ dissociated in water. Other kind of IPMCs - ionic liquid based, do not need wet environment for operating. A sheet of an ionic polymer is coated with a thin metal layer, usually platinum or gold. All freely movable cations inside the polymer migrate towards an electrode due to applied electric field, causing expansion of the material at the one end of the sheet and contraction at the other end, which results in bending of the sheet.

For simulating actuation of an IPMC sheet we need to solve coupled problems due to the complex nature of bending of an IPMC. It includes simulations in different domains such as mechanical, electrostatic and mass transfer, and even electrochemical for more advanced models. Some authors like Wallmersperger[2] and Nemat-Nasser[3] have already simulated mass transfer and electrostatic effects. We have used similar approach in our model. However, new approach is introduced in simulations of mechanical bending of an IPMC strip. By coupling equations from different domains, we get a Finite Element model for an IPMC muscle sheet accurate enough. It allows us to use the model as a starting point for solving more complex problems, thus we have also introduced a simulation of electrochemical reactions on the platinum electrode of an IPMC sheet which leads to self-oscillating actuation.
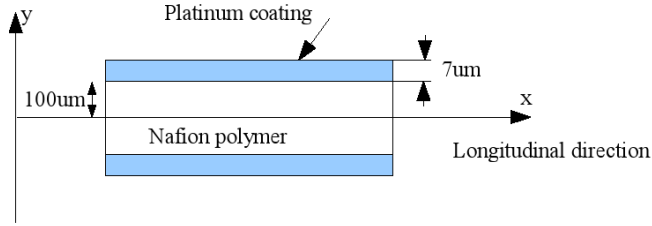
Figure 1. Illustration of domains and dimensions used in modeling.

1.1. Electrochemical oscillations

Spontaneous oscillations are common fenomena in nature and have been studied in many experiments, including electrochemical systems such as oxidation of organic materials and metals.[4] Electrochemical systems exhibiting instabilities often behave like activator-inhibitor systems, where the potential of an electrode is an essential variable and takes the role of the activator or of the inhibitor. Under certain conditions the system can generate oscillations.[5] We have conducted series of tests, where IPMC sheet have been immersed into acidic formaldehyde (HCHO) solution and exposed to a constant potential. The measurements however show current oscillations, which in turn result in oscillating bending of the IPMC sheet. Hence we have also introduced a model in this paper for describing such electrochemical systems.

2. SIMULATION DETAILS

An IPMC sheet consists of a backbone polymer and a metal coating. We have used Nafion^{TM} 117, coated with thin layer of platinum in our experiments. Mass transfer and electrostatic simulations are done in one mechanical domain - backbone polymer. Platinum coating is considered only in mechanics domain when calculating bending. So there are three mechanical domains as shown in Figure 1.

Most simulations are done for an IPMC strip, $1.5cm$ long, $200\mu m$ thick polymer coated with $7\mu m$ thick platinum, in a cantilever configuration - one end of the strip is fixed. Gravitational forces are not considered in any of the following simulations.

2.1. Migration of cations

Nernst-Planck equation describes diffusion, convection and in presence of electric field and charges, migration of particles. The general form of the equation is

$$\frac{\partial C_i}{\partial t} + \nabla \cdot (-D_i \nabla C_i - z_i \mu_i F C_i \nabla \phi) = -\vec{u_i} \cdot \nabla C_i, \tag{1}$$

where subscript i denotes different species, C is concentration, μ mobility of species, D diffusion constant, T absolute temperature, R gas constant, F Faraday constant, $\vec{u}$ velocity, z charge number and ϕ electric potential. This equations must be solved only for free cations. As voltage is applied to the electrodes of an IPMC, all free cations start migrating towards cathode, causing current in the outer electric circuit. As ions cannot move beyond the boundary of the polymer, charges start to accumulate, resulting in increase of electric field in the opposite direction to the applied one and it could be described by Gauss' Law:

$$\nabla \vec{E} = \frac{F \cdot \rho}{\varepsilon}, \tag{2}$$

where ρ is charge density, ε is absolute dielectric constant and E is the strength of the electric field and can be also expressed as $\nabla \phi = -\vec{E}$. A steady state of the cations forms when electric field created by distribution of cations cancels out applied electric field, i.e. the strength of electric field inside the polymer is approximately zero as shown in Figure 2. The steady state cation concentration of $1200 \frac{mol}{m^3}$ is shown in Figure 3. It is interesting to notice that there are fluctuations in charge distribution only in really thin boundary layers. There is no charge imbalance inside the polymer.
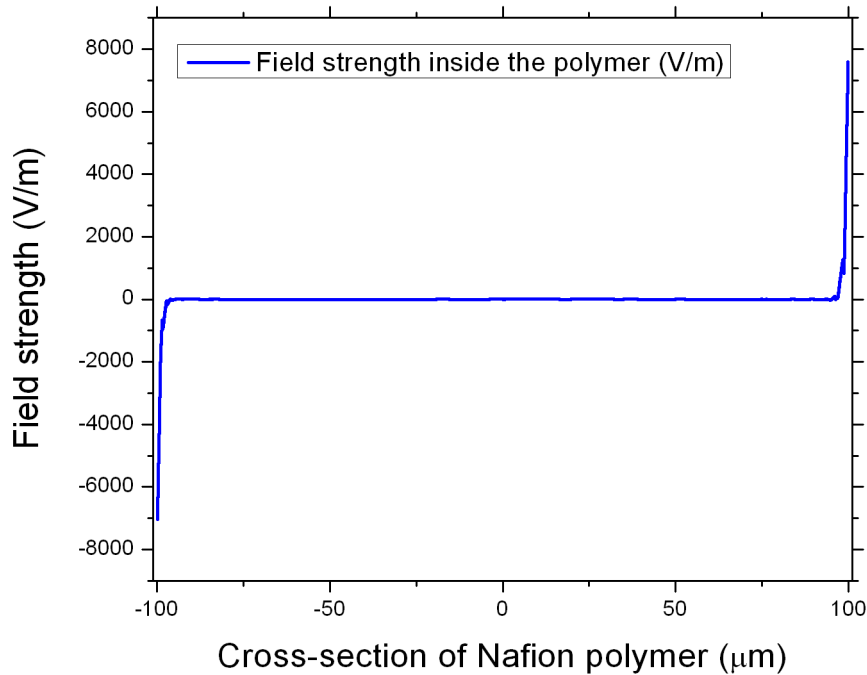
Figure 2. Electric field strength inside the IPMC in charge balance state. Notice that the field is zero inside the polymer, except in a really thin boundary layer.

2.2. Modeling actuation of an IPMC

Many authors like Shahinpoor[6] and Lee[7] have used cantilever beam equation to model bending of an IPMC strip in cantilever configuration. Though it describes position of the IPMC quite accurately for small displacements, it is not dynamical model - it does not show motion of the material in time. So using static Euler theory does not lead to really accurate time dependent model. Hence different approach is used for bending model: stiffness will be also considered when calculating. Importance of viscoelacity have been brought out also by some other authors like Richardson[8] and Newbury.[9]

2.2.1. Assumptions about bending mechanism

There are differences in charge distribution only in really thin boundary layers as we brought out before. General conclusion by many authors is that locally generated charge imbalance nearby platinum electrodes is directly connected to the bending of an IPMC.[10] As it worked out very well for our model, we followed the example of Leo[11] and defined longitudinal force per unit area in each point in the polymer of an IPMC as follows:

$$\vec{F} = (A \cdot \rho + sgn(\rho) \cdot B \cdot \rho^2) \cdot \hat{x}, \tag{3}$$

where ρ is charge density and A and B are constants which could be found from different experiments. $sgn(\rho)$ is to preserve correct sign of excess charge. The longitudinal force depends on the charge density in our model. The shape of the force inside the polymer is also shown in Figure 3.

2.2.2. Mathematics behind the bending

Finite Element method for solving physical equations is a very powerful tool and permits us to get better results than by using analytical models. We used structural mechanics equations described in Comsol Multiphysics
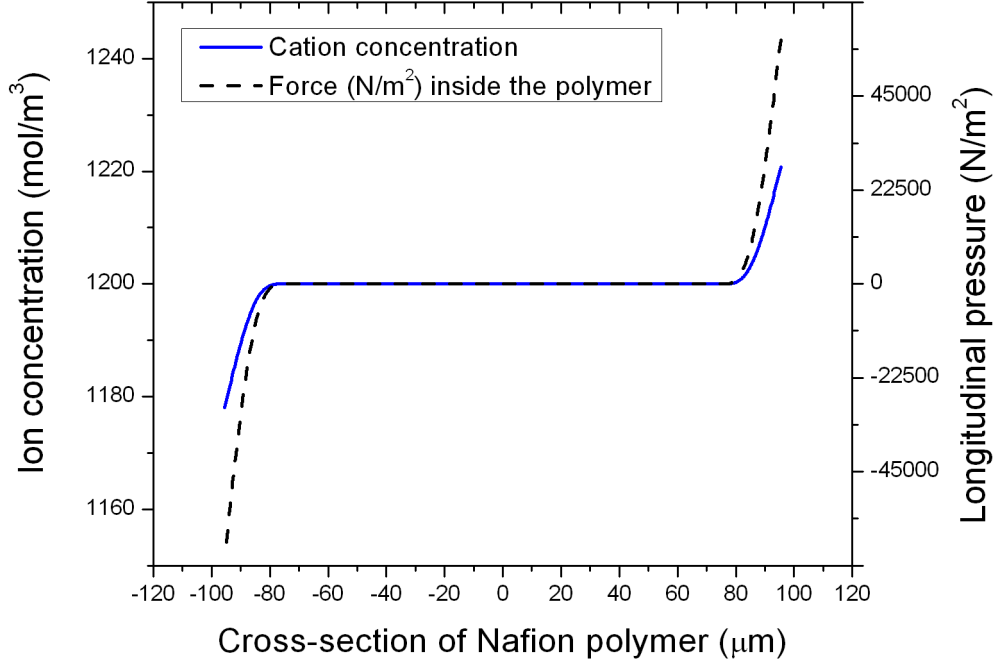
Figure 3. Cation distribution in a charge balance state. Also modeled longitudinal force inside the polymer is shown. Notice that force grows faster near the boundaries of the polymer than cation distribution. The reason for that is quadratic term in force formula as shown in Eq. 3. It is important to notice that the graph is somehow illustrative because real simulation maximum values for concentration and specially for stress are larger.

software package. Normal and shear strains are defined:

$$\varepsilon_i = \frac{\partial u_i}{\partial x_i}, \ \varepsilon_{ij} = \frac{1}{2}\left(\frac{\partial u_i}{\partial x_j} - \frac{\partial u_j}{\partial x_i}\right). \tag{4}$$

where u is the displacement, x denotes a coordinate and indices i and j are from 1 to 3 and denote components corresponding to x, y or z direction. As an IPMC sheet in our simulations is allowed to move only in x-y plane, $\varepsilon_3 = 0$ and $\varepsilon_{23} = \varepsilon_{13} = 0$. Considering this we can write symmetric strain tensor in vector form and symmetric stress tensor in vector form as follows:

$$\varepsilon = \begin{bmatrix} \varepsilon_1 \\ \varepsilon_2 \\ 0 \\ 2\varepsilon_{12} \\ 0 \\ 0 \end{bmatrix}, \ \sigma = \begin{bmatrix} \sigma_1 \\ \sigma_2 \\ \sigma_3 \\ \tau_{12} \\ \tau_{23} \\ \tau_{13} \end{bmatrix}, \ \tau_{ij} = \tau_{ji}. \tag{5}$$

The stress-strain relationship is

$$\sigma = D\varepsilon. \tag{6}$$

D is 6 x 6 elasticity matrix and consists of components of Young's modulus and Poisson's ratio. The system is in equilibrium if the following equation is satisfied:

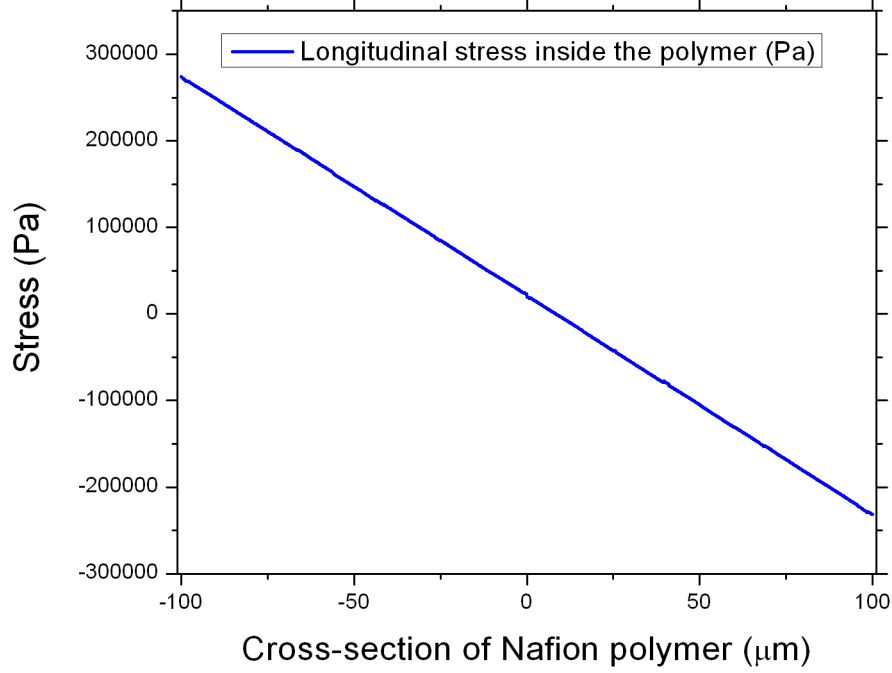$$-\nabla \cdot \sigma = \vec{F}, \tag{7}$$

Figure 4. Longitudinal stress inside the polymer backbone in global coordinates.

which is basically Navier's equation for displacement. For instance, stress generated in the polymer is shown in Figure 4. The stress inside the platinum coating is very much bigger, thus it is not shown in the figure.

2.2.3. Transient analysis of bending

As our simulations are rather dynamic than static, we have to introduce an equation to describe the motion of an IPMC sheet. To do that, we use Newton's Second law

$$\rho \frac{\partial^2 \vec{u}}{\partial t^2} - \nabla \cdot c \nabla \vec{u} = \vec{F}, \tag{8}$$

where the second term is static Navier's equation. Dynamic part is introduced by the first term of the equation. However, Eq. 8 describes a system without considering damping.

Motion with Rayleigh damping model for a system with a single degree of freedom can be described

$$m \frac{d^2 u}{dt^2} + \xi \frac{du}{dt} + ku = f(t), \tag{9}$$

where ξ is damping parameter and can be expressed $\xi = \alpha m + \beta k$. Parameter m is mass and k is stiffness and α and β are corresponding damping coefficients. Comsol Multiphysics uses a similar form for systems with multiple degrees of freedom:

$$\rho \frac{\partial^2 \vec{u}}{\partial t^2} - \nabla \cdot \left[c \nabla \vec{u} + c \beta \nabla \frac{\partial \vec{u}}{\partial t} \right] + \alpha \rho \frac{\partial \vec{u}}{\partial t} = \vec{F}, \tag{10}$$

where c is a constant used in Navier's equation, in static analysis, $\vec{u}$ displacement, ρ material density.

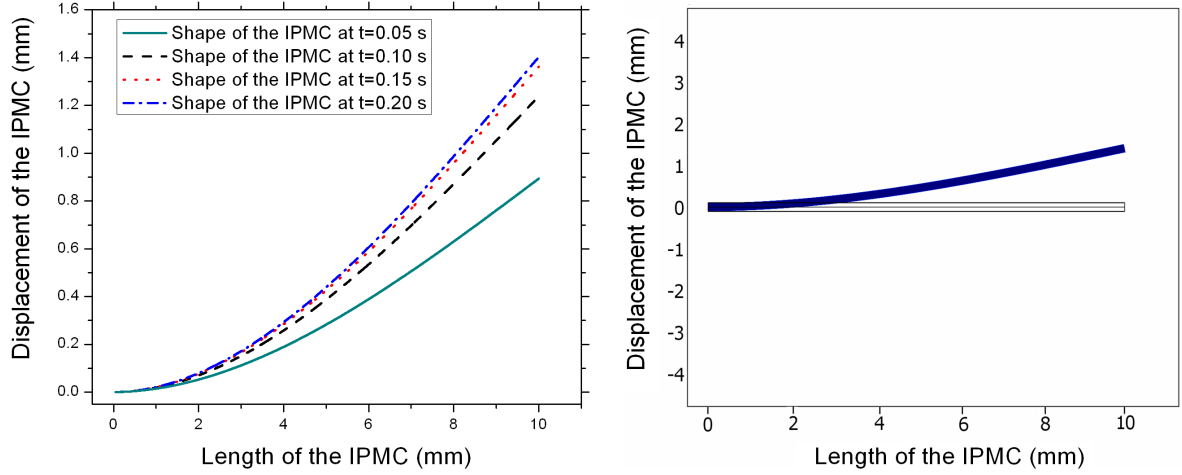All values used to simulate previously described equations are shown in Table 1.

Figure 5. On the left: the shape of an IPMC muscle at different times (simulated with 2V, 1cm long strip). On the right: illustration of bending at t=0.2s (snapshot).

Variable	Value	Dimension	Comment
D_{cation}	$2 \cdot 10^{-9}$	$\frac{m^2}{s}$	Diffusion coefficient of cations, e.g Na+.
ε	$3.8 \cdot 10^{-5}$	$\frac{F}{m}$	From capacitance measurment of an IPMC.
μ	$8 \cdot 10^{-13}$	$\frac{mol \cdot s}{kg}$	From Nernst-Einsten relation $\mu = \frac{D}{R \cdot T}$ where $T = 293K$, $R = 8.31 \frac{J}{mol \cdot K}$.
Y_N	$50 \cdot 10^6$	Pa	Young modulus of Nafion^{TM}.
Y_{Pt}	$169 \cdot 10^9$	Pa	Young modulus of platinum.
ρ_N	2600	$\frac{kg}{m^3}$	Density of Nafion^{TM}.
ρ_{Pt}	21500	$\frac{kg}{m^3}$	Density of platinum.
A	$5 \cdot 10^5$	$\frac{N \cdot m}{C}$	A constant in Eq. 3.
B	$3 \cdot 10^4$	$\frac{N \cdot m^4}{C^2}$	A constant in Eq. 3.
α	1	$\frac{1}{s}$	Mass damping parameter.
β	0.5	s	Stiffness damping parameter.

Table 1. Values used in simulations.

2.3. Results of simulations

Although there are couple of parameters in Eq. 3, which depend on experimental results and are not very uniquely specified for all IPMC sheets, the simulation results predict the bending of an IPMC sheet precisely enough to be used in further modeling problems. There are illustration of bending and a graph shown in Figure 5. As we are not modeling static problem, the time dependence of tip displacement of an IPMC muscle is shown in Figure 6.

By coupling previously described equations, we have developed a good basic model. Now it is possible to extend it by adding more equations to get physically meaningful results for more complicated problems. Next subsection of the article gives good example, because electrochemical reactions, which lead to self-oscillation of an IPMC muscle, are described and related to the basic model there.

2.4. Self-oscillations - coupling a problem of electrochemistry

We have conducted a series of tests with IPMCs in a constant electric field in formaldehyde (HCHO) solution. Measurements show that current oscillations begin from applied potential of ca. $0.75V$. Initial burst of current
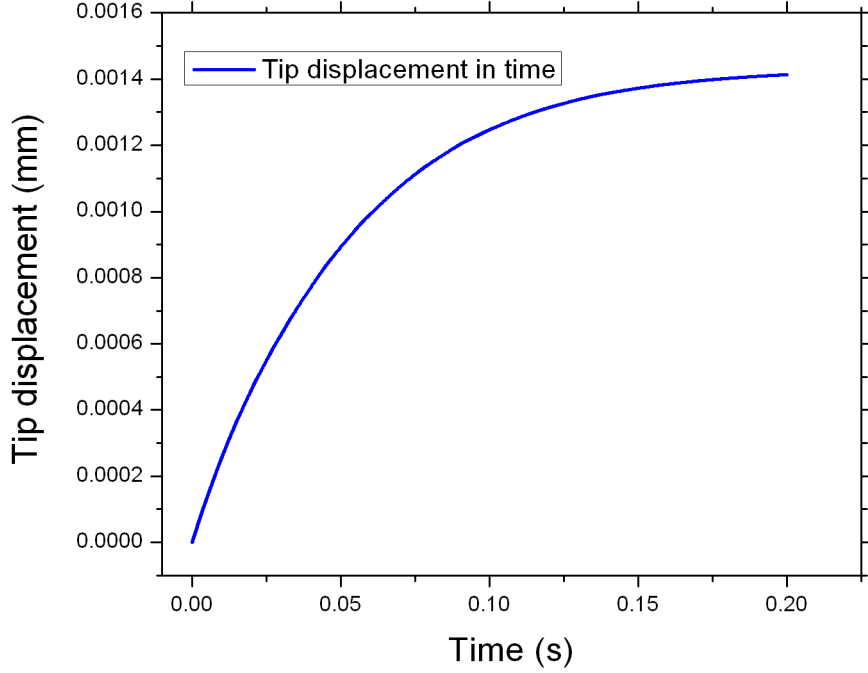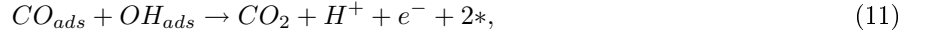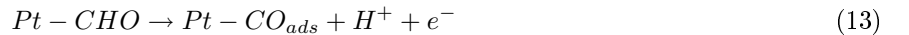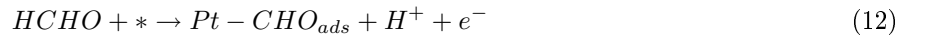
Figure 6. Tip displacement of an IPMC muscle in time.

is caused by the reaction

$$CO_{ads} + OH_{ads} \rightarrow CO_2 + H^+ + e^- + 2*, \tag{11}$$

where ads denotes species adsorbed to the surface of platinum and * denotes an active platinum site. The result of this reaction is freeing up 2 sites which causes CO to adsorb again. These reactions lead to oscillating potentials which in turn lead to self-oscillating motion of an IPMC.

Chronopotentiometry scans show that before Eq. 11, following reactions occur:

$$HCHO + * \rightarrow Pt - CHO_{ads} + H^+ + e^- \tag{12}$$

$$Pt - CHO \rightarrow Pt - CO_{ads} + H^+ + e^- \tag{13}$$

$$H_2O + * \leftrightarrow Pt - OH_{ads} + H^+ + e^- \tag{14}$$

HCHO is dissociated on the electrode surface at lower anodic potential. Higher anodic potential causes dehydrogenation of water which results in water oxidation with intermediate (Pt-OH) formation.

2.4.1. Simulating electrochemical reactions

It is shown by Strasser[12] that concentration of HCHO near the platinum surface is important for reaction 12 and it is an important variable for altering frequency of oscillations. We introduce a double layer near the surface of an electrode in our simulation model. Based on reactions 11 to 14 and conducted chronopotentiogram measurements we have developed equations to describe adsorption, desorption, reaction of species and voltage
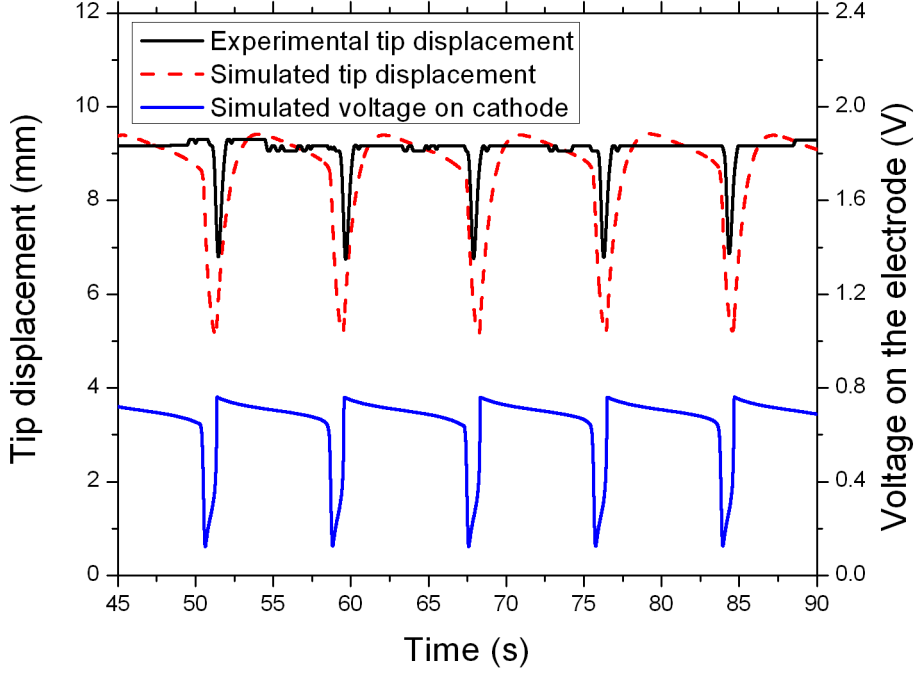
Figure 7. Simulation of voltage and tip displacement for 3M solution of HCHO + 3M H_2SO_4 and corresponding experimental data.

fluctuation on cathode:

$$\dot{\theta}_{CO} = k_2(1 - \theta_{CO} - \theta_{OH}) - k_4\theta_{CO}\theta_{OH} \tag{15}$$

$$\dot{\theta}_{OH} = k_3(1 - \theta_{CO} - \theta_{OH}) - k_3\theta_{OH} - k_4\theta_{CO}\theta_{OH} \tag{16}$$

$$\dot{E} = \frac{1}{C_{dl}}\left[I_{th} + (I - I_{th})\frac{c}{c_{2M}}sgn(c - c_{2M}) - jS_{pt}(k_1(1 - \theta_{OH} - \theta_{CO}) + k_4\theta_{OH}\theta_{CO})\right] \tag{17}$$

$$k_i = exp(s_i(E - E_i)) \tag{18}$$

Here θ is adsorption coverage of corresponding species and is normalized to 1, E is potential on cathode, I_{th} threshold current and equals to 10mA , I applied current, c concentration of HCHO near the electrode, c_{2M} equals $2000\frac{mol}{m^3}$ and s_i and E_i are correspondingly simulation parameters and reaction potentials as described by D. Kim.[13] Double layer conductivity C_{dl} and maximum adsorption coverage S_{pt} are taken equal to 1 in our simulations.

First version of this model was proposed in dissertation of D. Kim.[13] We have added second term to the Eq. 17, which brings in voltage dependence of concentration. As there is bigger concentration of HCHO near the electrode, there is also bigger current caused by direct oxidation of HCHO[12] - which is described by second term in Eq. 17. By coupling those equations with our base bending model, we get oscillating voltage and bending as shown in Figure 7. We can also vary concentrations of HCHO in the range of 1 to 3 $\frac{mol}{l}$ and still get simulation results reflecting experimental values.

Though the effect of double layer concentration according to current simulations turned out to be really small, further models should consider it more significantly. It would probably help us to improve model dependance of applied voltage/current and would be physically more accurate.

3. CONCLUSIONS

We have developed a Finite Element model for an IPMC sheet. Physical accuracy, flexibility and power of Finite Element method allows us to use this model as a base for coupling different equations corresponding to more complicated problems, such as was shown in the last subsection - electrochemical oscillations which occur on the surface of an electrode.

4. FUTURE WORK

Though the model we have developed has been accurate enough for current simulations, it could be developed further. The effect of water dragged by ions is not explicitly taken into account in current research, but to make Eq. 3 physically more meaningful, this effect should be described more precisely for future simulations. The effect of surface resistance change due to bending of IPMC sheet is not considered in current model, but it could be taken account in the future.

Equations describing electrochemical oscillations also need some revision, especially for making them more dependent on physical variables such as applied potential and concentration of formaldehyde in the double layer.

REFERENCES

1. M. Shahinpoor and K. Kim, "Ionic polymer-metal composites. I- Fundamentals," *Smart Materials and Structures* **10**(4), pp. 819–833, 2001.
2. T. Wallmersperger, B. Kröplin, and R. Gülch, "Coupled chemo-electro-mechanical formulation for ionic polymer gels—-numerical and experimental investigations," *Mechanics of Materials* **36**(5-6), pp. 411–420, 2004.
3. S. Nemat-Nasser and S. Zamani, "Modeling of electrochemomechanical response of ionic polymer-metal composites with various solvents," *Journal of Applied Physics* **100**(6), pp. 64310–64310, 2006.
4. B. Miller and A. Chen, "Oscillatory instabilities during the electrochemical oxidation of sulfide on a Pt electrode," *Journal of Electroanalytical Chemistry* **588**(2), pp. 314–323, 2006.
5. K. Krischer, "Spontaneous formation of spatiotemporal patterns at the electrode| electrolyte interface," *Journal of Electroanalytical Chemistry* **501**(1), pp. 1–21, 2001.
6. M. Shahinpoor, "Electro-mechanics of iono-elastic beams as electrically-controllable artificial muscles," *Artificial Muscle Research Institute, School of Engineering & School of Medicine, University of New Mexico, Albuquerque, New Mexico* **87131**.
7. S. Lee, H. Park, and K. Kim, "Equivalent modeling for ionic polymer–metal composite actuators based on beam theories," *Smart Mater. Struct* **14**, pp. 1363–8, 2005.
8. R. Richardson, M. Levesley, M. Brown, J. Hawkes, K. Watterson, and P. Walker, "Control of Ionic Polymer Metal Composites," *IEEE/ASME Transactions on Mechatronics* **8**(2), p. 245, 2003.
9. K. Newbury, *Characterization, Modeling, and Control of Ionic Polymer Transducers*. PhD thesis, Virginia Polytechnic Institute and State University, 2002.
10. S. Nemat-Nasser and J. Li, "Electromechanical response of ionic polymer-metal composites," *Journal of Applied Physics* **87**(7), p. 3321, 2000.
11. D. Leo, K. Farinholt, and T. Wallmersperger, "Computational models of ionic transport and electromechanical transduction in ionomeric polymer transducers," *SPIE proceedings series* , pp. 170–181.
12. P. Strasser, M. Eiswirth, and G. Ertl, "Oscillatory instabilities during formic acid oxidation on Pt (100), Pt (110) and Pt (111) under potentiostatic control. II. Model calculations," *Journal of Chemical Physics* **107**(3), pp. 991–1003, 2006.
13. D. Kim, *Electrochemically Controllable Biomimetic Actuator*. PhD thesis, University of Nevada, Reno, 2006.